Metastable *M* center in InP: Defect-charge-state–controlled structural relaxation

M. Levinson, M. Stavola, J. L. Benton, and L. C. Kimerling
AT&T Bell Laboratories, Murray Hill, New Jersey 07974
(Received 13 June 1983)

The *M* center is an unusual metastable defect which can exist in either of two configurations, each with distinct electronic properties. These properties, together with the thermally stimulated configurational transformation kinetics, lead to a model of charge-state–controlled structural relaxation involving a shallow-donor–intrinsic-defect complex. We present studies of the electronically and optically stimulated configurational transformations. These include unique pulsed optical experiments, which are made possible by the particular properties of the defect, and which provide information on the rate of lattice relaxation associated with the transformation. The results lead to a more complete understanding of the nature of the configurational instability for the *M* center than for any other covalent semiconductor defect exhibiting large lattice relaxation.

I. INTRODUCTION

We have recently reported the observation of an unusual metastable defect in 1-MeV-electron–irradiated undoped n-InP.[1,2] This defect, which we call the *M* center, for metastable, was shown to exist in either of two configurations, *A* or *B*, depending on its charge state. Each configuration is characterized by distinct deep-level transient-capacitance (DLTS) spectra and thermally stimulated capacitance behavior. The kinetics of the thermally activated transformations between the two configurations were shown to be governed by thermally activated electron capture and emission. As a result, either configuration may remain metastable at low temperature ($T \lesssim 160$ K).

This defect appears to be similar to several other anomalous defects, previously reported in covalent semiconductors, which undergo large lattice relaxation.[3,4] These defects include the *DX* center responsible for persistent photoconductivity in AlGaAs (Refs. 5 and 6) and GaAsP,[7] the EL2 defect associated with photocapacitance quenching in GaAs,[8–10] and a metastable defect in Si.[2,11] These systems have usually been described with the help of one-dimensional configuration-coordinate diagrams. Unfortunately, the exact nature of the electron-lattice interaction, which provides the driving force for configurational change, is not well defined.[3,4] In addition, in the case of EL2 in GaAs, this approach is unsuccessful in explaining the "Auger deexcitation" of the photocapacitance quenching.[9,10,12]

Unlike these other defects, both configurations of the *M* center may be directly observed by DLTS. This characteristic permits detailed studies of the properties of the defect in both configurations, as well as the kinetics of the transformations between configurations. We are thus able to provide strong evidence for a model which invokes an electrostatically driven structural rearrangement of the defect.[1] The particular atomic arrangement of each configuration gives rise to distinct electronic and optical properties.

The DLTS spectra for both configurations are shown in Fig. 1. Our notation and related information from Ref. 1 are included in Table I. We have shown[1] that when the defect electronic states are fully occupied, the defect is in configuration *A*. When three electrons are lost, configuration *B* is formed according to the reaction

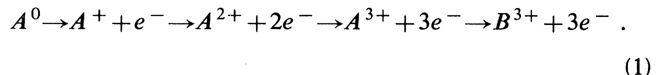

$$A^0 \rightarrow A^+ + e^- \rightarrow A^{2+} + 2e^- \rightarrow A^{3+} + 3e^- \rightarrow B^{3+} + 3e^- . \quad (1)$$

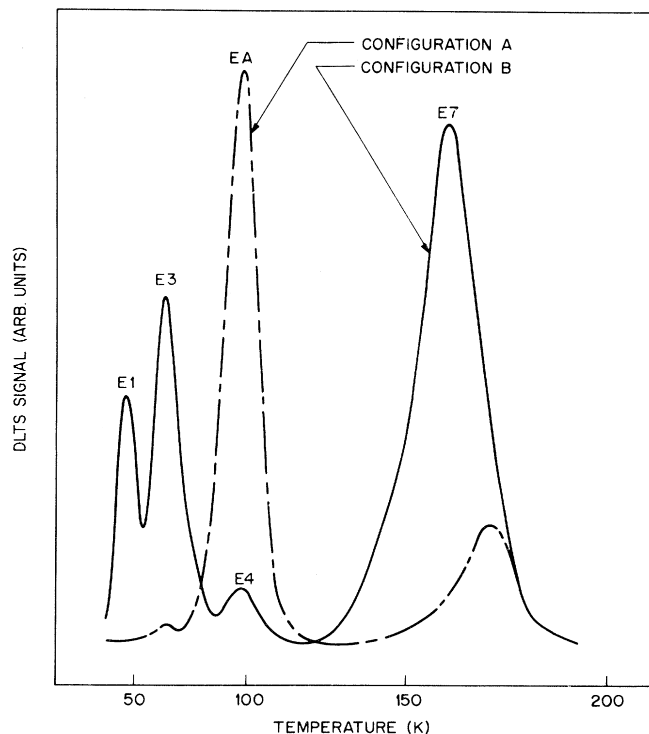

FIG. 1. DLTS spectra of irradiated material showing the result of cooling with the bias off (configuration *A*) and with applied reverse bias (configuration *B*). DLTS rate window of 123 s^{-1}.

 ©1983 The American Physical Society

TABLE I. Summary of energy levels, charge states, and observed electronic transitions for configurations A and B.

Highest occupied energy level	Charge state	Model	Transition	Order	Electron emission: Thermal DLTS	Electron emission: Thermal E_{act}	Electron emission: Optical	Hole capture
A_1	A^0	$(C^-D^+)^0$	$A^0 \rightarrow A^+$	first	EA	0.15 eV	e^0_{n1}	first
A_2	A^+	$(C^-D^+)^+$	$A^+ \rightarrow A^{2+}$	second	(TSCAP)	$\sim$0.4 eV	e^0_{n2}	second
A^*	A^{2+}	$(C^-D^+)^{2+}$	$A^{2+} \rightarrow A^{3+}$	third	(TSCAP)	$\sim$0.4 eV	e^0_{n3}	third
	A^{3+}	$(C^-D^+)^{3+}$	A^{3+} transforms to B^{3+}					
B_1	B^+	C^0+D^+	$B^+ \rightarrow B^{2+}$		$E1, E3$	0.09, 0.14 eV	not investigated	
B_2	B^{2+}	$C^+ + D^+$	$B^{2+} \rightarrow B^{3+}$		$E7$	0.37 eV	not investigated	
	B^{3+}	$C^{2+}+D^+$						

Thermal emission of the first electron is seen as DLTS peak EA. The thermal emissions of the second and third electrons appear to occur simultaneously with activation energies of $\sim$0.4 eV, and result in the transformation to B. The transformation $A \rightarrow B$ was also shown to occur as a result of hole capture by A.

The defect in configuration B can gain two electrons,

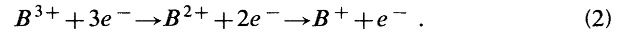

$$B^{3+}+3e^- \rightarrow B^{2+}+2e^- \rightarrow B^+ + e^- \ . \quad (2)$$

The first electron captured corresponds to the inverse of the emission responsible for DLTS peak $E7$. Likewise the second capture corresponds to the inverse of $E1$ or $E3$. [The splitting resulting in the two peaks $E1$ and $E3$ is evidently due to two different varieties of the defect which have slightly different activation energies for electron emission in configuration B ($E1$ and $E3$) but behave similarly when in A, as shown by peak EA.] Electron capture also appears to control the transformation $B \rightarrow A$. The thermally activated nature of this electron capture is responsible for the metastability of B in the presence of free electrons at $T \lesssim 150$ K.

A charge-state-controlled, electrostatically driven, structural rearrangement of an intrinsic defect or defect complex C, and a shallow donor D can be used to model the data. For simplicity, this rearrangement can be conceptualized in the following way: The two species are paired when C is occupied (configuration A), and as C becomes positive they dissociate to form configuration B (consistent with Eq. 1) as

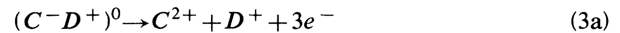

$$(C^-D^+)^0 \rightarrow C^{2+}+D^+ + 3e^- \quad (3a)$$

or

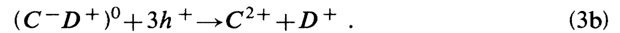

$$(C^-D^+)^0 + 3h^+ \rightarrow C^{2+}+D^+ \ . \quad (3b)$$

The two defects remain sufficiently close together that when C becomes negative they reassociate as $B \rightarrow A$,

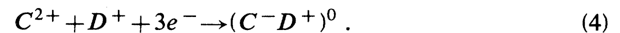

$$C^{2+}+D^+ + 3e^- \rightarrow (C^-D^+)^0 \ . \quad (4)$$

Here the controlling electron capture is that of a third electron B^+/B^0.

In this paper we describe the effects of continuous and pulsed optical excitation, and minority-carrier (hole) injection on the transformations. The results are consistent with the original model and yield additional insights into the nature of the defect. In particular, pulsed optical measurements allow study of processes which are not observable with normal junction capacitance and photocapacitance methods, such as that of the lattice relaxation rate associated with configurational change.

II. EXPERIMENTAL

The p^+n mesa diodes used in this study consisted of liquid-phase epitaxial p^+ layers on nominally undoped liquid-encapsulated Czochralski-grown n-InP substrates.[1] C-V measurements indicated a free-carrier density $n = 3\times10^{15}$ cm^{-3}. 1-MeV-electron irradiations were performed at room temperature to a total fluence of 10^{16} cm^{-2}, and the samples exhibited the characteristic radiation-defect spectrum,[13] including the metastable de-

fects as previously reported.[1,2] The samples were annealed for 1 h at 180 °C to eliminate defects $E6$ and $E8$.[13] DLTS measurements were made using the standard lock-in amplifier technique.

The basic procedure[1,2] used in these measurements was to set the defect in the desired configuration by cooling from $T > 200$ K to low temperature either at zero bias (configuration A) or with an applied reverse bias (configuration B). The junction was then optically or electrically (hole-injection) stimulated, and DLTS measurements were performed to observe any change in peak heights that would correspond to a transformation from one configuration to the other. Because of the extreme sensitivity of the transformation to hole injection, switching transients were avoided at low temperature by adjusting the bias only with potentiometers and performing all circuit modifications at zero bias.

Variable-wavelength illumination was introduced through the side of the mesa diodes by a tungsten source and grating monochromator. A pyroelectric radiometer was used to measure light intensity at each wavelength, and the optically induced transformation rates were normalized accordingly. Measurements at higher intensity were made using both a continuous and a pulsed neodymium:yttrium-aluminum-garnet (Nd:YAG) laser operating at 1.06 μm. Absolute intensity calibration was not possible due to uncertainty involving the coupling of the light into the mesa structures. However the incident intensities were $\sim 10^{-4}$ W cm^{-2} for the monochromator and up to 4 W cm^{-2} for the continuous laser.

Hole injection was accomplished with a constant nanoampere source operated in forward bias. In all cases the sample temperature was controlled to within ± 0.2 K during illumination or injection.

III. OPTICAL EFFECTS

A. Continuous illumination

Subband-gap light was found to promote the transformation $A \rightarrow B$ at temperatures below the thermally activated transition. Figure 2 shows peak height EA (which is proportional to the concentration of configuration A) versus time of illumination. This process is due to optically stimulated electron emission and confirms the interpretation of the thermally activated transformation as being controlled by thermal electron emission. However, the reverse transition $B \rightarrow A$ was not observed for any of the photon energies used, $0.56 \leq h\nu < 1.24$ eV, or for high intensity at $h\nu = 1.17$ eV.

Three electrons are lost in the transformation $A \rightarrow B$ so the optically stimulated reaction can be expressed [consistent with Eq. (1)] as

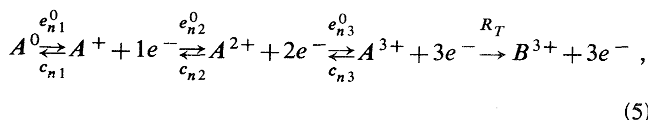

$$A^0 \underset{c_{n1}}{\overset{e_{n1}^0}{\rightleftarrows}} A^+ + 1e^- \underset{c_{n2}}{\overset{e_{n2}^0}{\rightleftarrows}} A^{2+} + 2e^- \underset{c_{n3}}{\overset{e_{n3}^0}{\rightleftarrows}} A^{3+} + 3e^- \overset{R_T}{\longrightarrow} B^{3+} + 3e^- , \quad (5)$$

where e_n^0 and c_n are rates of optically excited electron emission and free-electron capture, and R_T is the rate of the lattice relaxation associated with the transformation.

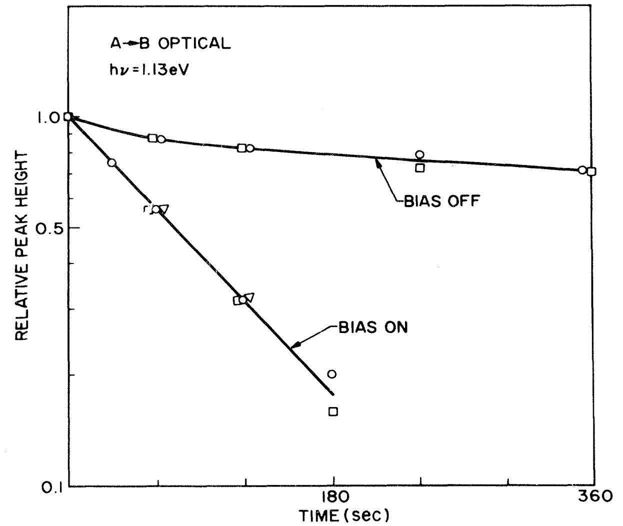

FIG. 2. DLTS peak height EA vs time of anneal under illumination, either with or without applied reverse bias. For each point, the defects are set in configuration A by cooling the sample from $T > 200$ K at zero bias. Illumination is then performed for the indicated time followed by a DLTS measurement. □ denotes illumination at $T = 101.6$ K, ○ denotes illumination at $T = 33.7$ K, and △ denotes bias applied at $T = 101.6$, cool, illumination at 33.7 K.

Once transformed, the defect remains in configuration B because the final electron capture required for the reverse transition is thermally activated and does not occur at temperatures $T \lesssim 150$ K.[1,2]

In general, the kinetics of the optically stimulated transformation are described by the solution of the five coupled linear first-order differential equations governing the temporal evolution of the quantities in Eq. (5), together with the appropriate boundary conditions. However, as shown below, either the second or third electron emission, e_{n2}^0 or e_{n3}^0, is rate limiting.

Typical curves of DLTS signal EA (which is proportional to the concentration of A) versus time of illumination are shown in Fig. 2 for both conditions of zero bias and applied reverse bias during illumination. Both curves are independent of temperature in the range investigated $31 < T < 100$ K. In the "bias-on" condition, the capture rates c_n are negligible as free electrons are swept out of the depletion region by the junction electric field. The bias-on curve of Fig. 2 shows a linear relation between logarithmic concentration of A and time. This relation is consistent with a simple first-order reaction, and therefore indicates that one step of Eq. (5) is rate limiting. The scatter of data may be used to estimate the maximum nonlinearity, and therefore that the rate-limiting step is at least an order of magnitude slower than any other step.

The first optical electron emission, corresponding to the thermal electron emission of DLTS peak EA, is not the rate-limiting step by the following reasoning. Peak EA appears at the temperature (~ 100 K) where the thermal emission time constant is equal to the DLTS rate window, which is on the order of milliseconds. Cooling the sample

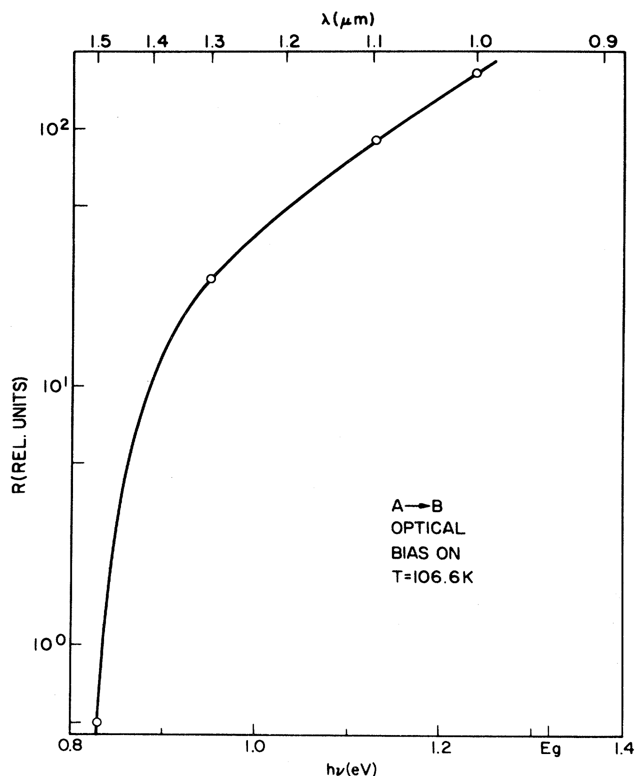

FIG. 3. Relative rates of the transformation $A \rightarrow B$ as a function of photon energy.

at zero bias to obtain configuration A and applying the reverse bias at or above this temperature thus allows the thermal emission of the first electron prior to illumination. If, however, the bias is applied at much lower temperature, then the first electron remains trapped. The results shown in Fig. 2 labeled "bias on" are identical for

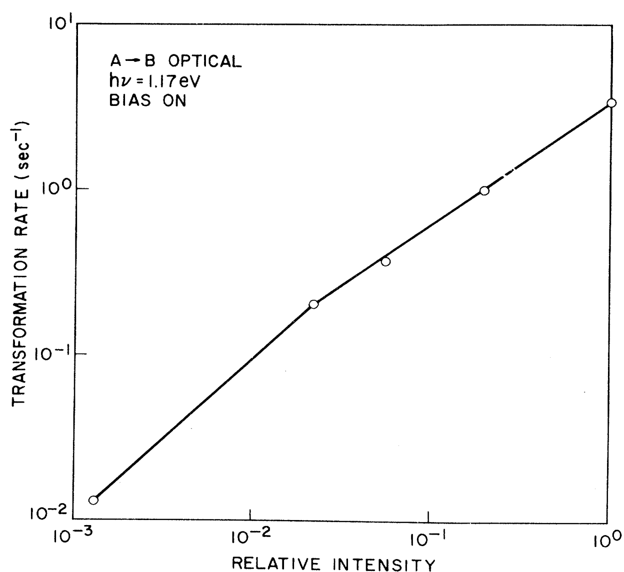

FIG. 4. Transformation rate $A \rightarrow B$ vs light intensity at 1.17 eV.

bias applied at both 101.6 and 33.7 K. Since the presence or absence of e_{n1}^0 does not affect the transformation rate, this emission process cannot be the rate-limiting step. This is further confirmed by the following experiment. The sample is cooled at zero bias in darkness to 101.6 K, where the bias is applied, and the first electron emitted. The sample is then cooled to 33.7 K and illuminated. The results (Fig. 2) are identical with those above. Therefore, either e_{n2}^0 or e_{n3}^0 is rate limiting.

The bias-on $A \rightarrow B$ transformation rate is shown as a function of photon energy in Fig. 3. The observed threshold at ~ 0.8 eV should be compared with the thermal activation energy of ~ 0.4 eV for the transformation.[1,2] This difference indicates a Frank-Condon shift for the electron emission process which controls the transformation. Figure 4 shows the intensity (I) dependence of the $A \rightarrow B$ transformation rate (R) at the YAG-laser energy of 1.17 eV, again with the reverse bias applied. The dependence is linear at low intensities, but becomes slightly sublinear at high intensities where $d(\ln R)/d(\ln I) \approx 0.75$. The low-intensity linear behavior provides the basis for the normalization of monochrometer output for the transformation-rate—versus—photon-energy data (Fig. 3) which was taken in that regime.

B. Pulsed illumination

1. Free-electron quenching effect

When illumination is performed at zero bias the transformation rate is slower and the concentrations no longer have simple exponential dependencies, as shown in the "bias-off" curve of Fig. 2. In this case, free electrons are available to be recaptured by the ionized defects before they transform to B, and the reaction is therefore partially "quenched." The optical ionization and free-electron capture processes can be separated in time by using pulsed illumination under reverse bias, in conjunction with bias-removing voltage pulses. This technique, in principle, permits time-resolved studies of the individual processes involved in the transformation. In particular, information may be gained about the lattice relaxation rate R_T.

The procedure is illustrated in Fig. 5. After cooling the sample at zero bias to set configuration A, the reverse bias is applied. A 10-ns optical pulse ($h\nu = 1.17$ eV) is used to ionize the defects with an intensity chosen so that a population is produced in each of the charge states A^{1+}, A^{2+}, and A^{3+}. Those defects in A^{3+} transform to configuration B at a rate R_T [Eq. (5)]. Additional light pulses result in continued ionization of those defects still in A^0, A^{1+}, and A^{2+}, and an increased concentration of B. However, if each light pulse is followed by a sufficiently long bias-removing voltage pulse, a partial quenching effect occurs as free electrons are captured and return those defects which remain in A^{1+}, A^{2+}, or A^{3+} to A^0. The proportion of defects which transform to B in this latter case can only be those which are ionized to A^{3+} during the light pulse and then transform before recapturing an electron. The transformed defects remain in configuration B because the electron capture required for the reverse transition is thermally activated and does not occur at

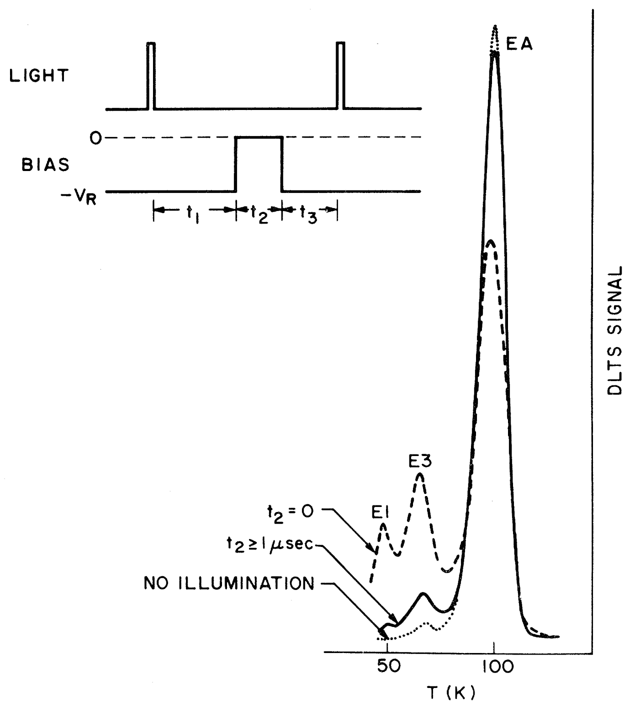

FIG. 5. Pulsed optical experiment showing the bias pulse "quenching" effect on the transformation $A \rightarrow B$. Data represents 3000 light pulses.

$T \lesssim 150$ K. This proportion can thus be detected in a subsequent DLTS measurement.

DLTS spectra are shown in Fig. 5 following 3000 light pulses, both with and without the bias-removing pulses. The quenching effect is clearly seen. The reaction quenching increases as expected for increasing bias-removing pulse widths t_2 and was found to saturate at $t_2^{sat} \approx 1\ \mu$s. (The value of t_2^{sat} and the variation of quenching as a function of t_2 have a complex dependence on light intensity, capture rates c_n, and the total number of pulses.)

2. Lattice relaxation rate

If the lattice relaxation rate R_T is less than the electron-capture rate c_{n3} (Eq. 5), then R_T can be resolved by measuring the extent of quenching as a function of bias pulse delay time t_1. t_1 represents the time available for A^{3+} to transform to B^{3+} before being exposed to free electrons. Therefore, a decrease in t_1 should lead to an increase in the proportion of A^{3+} which recapture an electron before transforming, therefore leading to an increase in quenching. The time resolution is then limited by c_{n3}.

In fact, no change in quenching was observed for all t_1 between 40 ns and 50 ms and temperatures between 33 and 150 K. Thus R_T is greater than c_{n3}. t_2^{sat} is determined by the capture rates c_n. Therefore $c_{n3} \geq (t_2^{sat})^{-1}$, and we may take a conservative lower limit for R_T as $(t_2^{sat})^{-1} = 10^6\ s^{-1}$. It is therefore apparent that all A^{3+} transforms quickly to B, and the reaction quenching effect seen in Fig. 5 is due to electron capture by A^{1+} and A^{2+} only.

If we assume that the lattice relaxation involves a diffusionlike atomic displacement with a vibrational attempt frequency of $\sim 10^{13}\ s^{-1}$, we have

$$10^6 < R_T = 10^{13} \exp(-E_a/kT) . \quad (6)$$

This relation, with $T = 33$ K, gives a conservative upper limit for any atomic displacement activation barrier $E_a < 0.046$ eV. This value is consistent with the observed lack of temperature dependence for the optically stimulated transition $A \rightarrow B$ (Fig. 2).

3. Energy levels in A

The lack of temperature dependence of the quenching effect can also be used to gain information on the order of energy levels in configuration A. Thermally stimulated capacitance (TSCAP) measurements have shown that the thermally activated transformation $A \rightarrow B$ occurs with the simultaneous emission of the second and third electrons at $T \approx 160$ K.[1] There are two possible explanations for this behavior: Firstly, the transformation could proceed upon loss of the second electron ($A^{1+} \rightarrow A^{2+}$), and the third would be emitted immediately afterwards because of a decreased emission activation energy in configuration B. (This latter emission would then correspond to DLTS peak $E7$.) Alternatively, the binding energy of the third electron in configuration A, E_3^b, may be equal to or less than that of the second, E_2^b. Consequently, a temperature sufficient to cause thermal emission of the second electron is also sufficient for emission of the third electron. The third emission thus immediately follows that of the second. This situation would correspond to a zero or negative correlation energy $U = E_3^b - E_2^b$.[14]

Although the analysis of the lattice relaxation rate experiment in the preceding section does not depend on which charge state of A controls the transformation, we have assumed that the transformation occurs at A^{3+} rather than at A^{2+}. This assumption can now be justified, and the second explanation above shown to be correct, by ruling out the first explanation. The reasoning is as follows: If the second electron were the controlling emission, then the lattice relaxation would occur at A^{2+}. The quenching effect would then be due to the capture $A^{1+} \rightarrow A^0$ only, because all the A^{2+}'s would transform before recapturing an electron. However, the experiment may be performed with all A in either A^0 or A^{1+} at the beginning of the light pulse. The latter condition occurs at temperatures where the first electron is emitted thermally ($A^0 \rightarrow A^{1+}$) during time t_3 (Fig. 5). This emission occurs when t_3 and the sample temperature are greater than or equal to the time constant and temperature of DLTS peak EA. It is found that the extent of quenching is the same for temperatures both well above and well below $T(EA)$. This result indicates that the quenching effect cannot be due to the capture $A^{1+} \rightarrow A^0$, because it makes no difference if the defect is returned to A^{1+} thermally before the next light pulse. Therefore, the quenching is due to capture by A^{2+}, so there must be a stable population in A^{2+} during time interval t_1 after the light pulse. Thus the transformation does not proceed until the third electron is lost and A^{3+} is achieved.

The second explanation is therefore correct and the zero or negative-U character may be examined by noting any decrease of the quenching effect with increasing temperature up to the second-electron thermal emission at $T \approx 160$ K. If the third electron is bound less strongly than the second (negative-U ordering), then it will be emitted thermally during time t_1 at $T < 160$ K from those defects which have already lost the second electron optically (assuming similar capture cross sections and thus exponential prefactors for thermal emission from A^{1+} and A^{2+}). This would result in an increased number of A^{3+}, and also more B, and thus reduced quenching. In fact, at $t_1 = 50$ ms and all $T \leq 150$ K there is no change in the extent of quenching, indicating that $E_2^b \approx E_3^b$. That is, the thermal emission activation energies are nearly equal.

IV. MINORITY-CARRIER EFFECTS

As previously reported,[1] hole injection induces the transition $A \rightarrow B$ consistent with Eq. (3b) but not the reverse $B \rightarrow A$. This behavior again confirms the charge-state-controlled nature of the transformation. Hole capture is equivalent in its effect on charge state to thermally or optically stimulated electron emission.

Figure 6 shows a typical variation of DLTS peak heights with time at constant injection current. Two distinct stages of the transformation are evident. In this case peaks $E1$ and $E3$ appear at the same rate, so there is no apparent relation between these two stages and the two stages previously reported for the thermally activated transition $A \rightarrow B$.[1] In the latter case, part of $E1$ appears in one stage near 110 K, and the remainder of $E1$ together with all of $E3$ in a second stage at ~ 160 K.

The dependence of transformation rate on injection current for both stages 1 and 2 are shown in Fig. 7. A good fit to the data is provided by taking $R \propto J^n$, where a least-squares analysis gives $n = 3.0$ for stage 1 and $n = 2.3$ for stage 2. The cubic current dependence of stage 1 is consistent with Eq. (3b), and confirms that three holes are captured in the transformation. The approximate square dependence of stage 2 implies two-carrier kinetics. Stage 2 thus appears to reflect a two step process where the first hole is captured quickly and the rate is determined by the capture of the second and third holes.

The temperature dependence of the rates in both stages are shown in Fig. 8. This data shows transformation rates for $J = 4 \times 10^{-4}$ A cm^{-2} and $33 < T < 50$ K which are 20–30 orders of magnitude faster than that calculated for the thermally activated $A \rightarrow B$ transition in this temperature range. The form of the curves is assumed to reflect the combined temperature dependence of the hole-capture cross section, hole lifetime, and injection ratio.

V. DISCUSSION

A. Energy-level structure

The energy levels for both configurations, which have been determined from the experimental data, are diagrammed in Fig. 9. The charge states and observable electronic transitions involving these levels are summarized in Table I. In configuration A the first, second, and third electrons are emitted from levels A_1, A_2, and A^*, respectively. The two observable electron emissions in

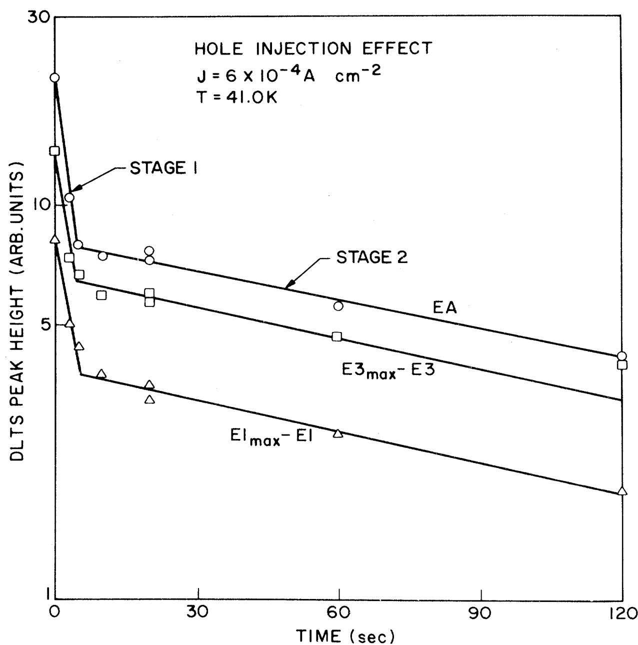

FIG. 6. DLTS peak heights vs time of hole injection showing the transformation $A \rightarrow B$. For each point, the defects are set in configuration A by cooling at zero bias, and the injection current is applied for the indicated time, followed by the DLTS measurement. ○ denotes EA, □ denotes $E3_{\max} - E3(t)$, and △ denotes $E1_{\max} - E1(t)$.

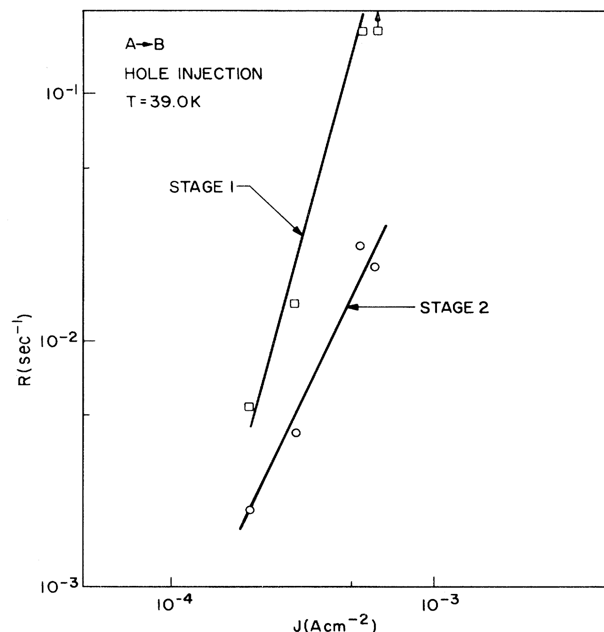

FIG. 7. Transformation rate $A \rightarrow B$ vs injection current density at $T = 39.0$ K.

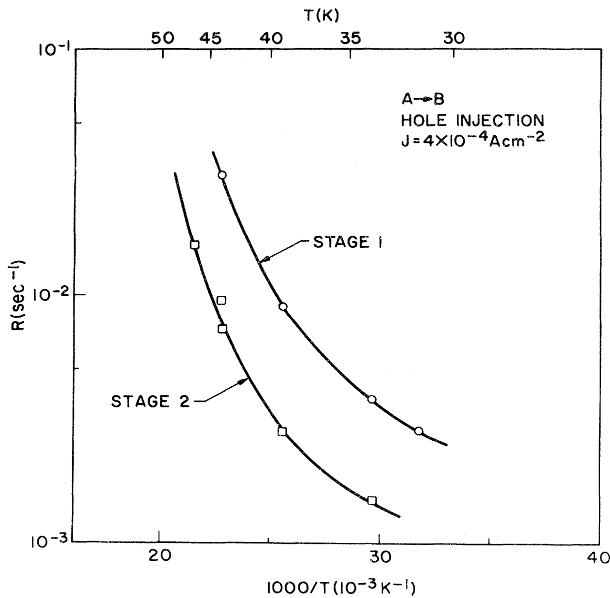

FIG. 8. Transformation rate $A \to B$ vs temperature. Injection current $J = 4\times10^{-4}$ A cm^{-2}.

configuration B are from levels B_1 and B_2. The transitions corresponding to DLTS peaks EA, $E1$ or $E3$, and $E7$, are indicated. A^* is the controlling level of the transformation $A \to B$, which occurs when A^* is unoccupied. The pulsed optical experiments show, for $A \to B$, that once the proper charge state is attained, the transformation proceeds with a negligible atomic displacement activation barrier.

The pulsed optical measurements also showed that A_2 and A^* are similar in energy position because the temperature for thermal electron emission is similar for both states. However, A^* uniquely controls the transformation and configuration A is stable independent of the occupation of A_2.

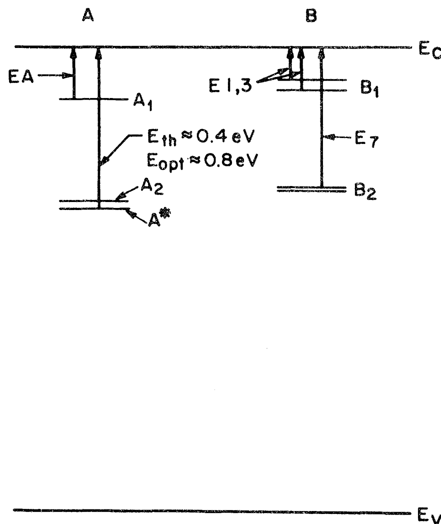

FIG. 9. Energy-level diagrams for configurations A and B.

B. Observation of configurational change

Analagous to A^*, we can represent the electron capture occurring with $B \to A$ by a transitional state B^*. The levels A^* and B^* are in a sense "hidden." This is because once they have emitted (A^*) or captured (B^*) an electron, they disappear as the defect transforms to the other configuration. Because the observation of a defect electronic state using junction spectroscopic techniques is accomplished by detection of a carrier emission from that level, B^* is essentially unobservable. It never emits an electron because upon filling it immediately disappears as B transforms to A. On the other hand, A^* is more amenable to study because one-electron emission may be observed as $A \to B$. Thus it does not appear in DLTS spectra (which require repetitive emissions), but can be observed by TSCAP.[1] It should be noted that configuration B can be metastable at zero bias because electron capture into B^* is thermally activated and does not occur at low temperatures.[1] If this capture process were not thermally activated, the DLTS spectrum of B would not be observed because B would disappear during each trap-filling pulse. However, in addition to peak EA, a DLTS peak corresponding to the emission from A^* would be seen. In this case, each trap-filling and emptying cycle would involve a transformation $B \to A \to B$, and the DLTS signal would appear as one peak with the electron emission characteristics of A^* and capture properties determined by configuration B.

The state labeled A_2 also does not give rise to a DLTS peak. This is due to the fact that coincidentally it is very close in electron thermal emission rate to A^*. At the temperature where A_2 would emit an electron, A^* also empties and configuration A transforms.

It is apparent that with somewhat different electronic properties of either or both configurations, this analysis would predict configurational transformations which are undetectable, or only partially detectable, using these experimental techniques. The EL2 center in GaAs appears to fall in the latter category.[12] Thus it is possible that charge-state-controlled structural relaxation may be a fairly common occurrence for defect complexes in covalent semiconductors, but these effects are not easily observed.

VI. CONCLUSION

We have characterized the electronic and optical properties of the M center in both of its configurations, and examined the transformations between configurations induced by electronic, thermal, and optical stimulation. The results can be simply and consistently explained by the model of electrostatically driven structural rearrangement of the defect, which produces two configurations, each with distinct electronic states. The characteristics of these states govern the observed properties of each configuration and the kinetics of their transformations. Certain of these properties are fortuitous in that they allow observa-

tion of each configuration by junction capacitance methods. We are thus lead to a more complete understanding of the configurational instability for the *M* center than for any other covalent semiconductor defect exhibiting large lattice relaxation.

ACKNOWLEDGMENTS

We are grateful to H. Temkin for providing samples, to H. L. Carter and K. B. Lyons for assistance with the pulsed optical measurements, and to G. A. Baraff for a critical review of the manuscript.

[1]M. Levinson, J. L. Benton, and L. C. Kimerling, Phys. Rev. B 27, 6216 (1983).

[2]J. L. Benton and M. Levinson, in *Defects in Semiconductors* II, edited by S. Mahajan and J. W. Corbett (North-Holland, New York, 1983), p. 95.

[3]J. M. Langer, J. Phys. Soc. Jpn. 49, Suppl. A, 207 (1980).

[4]J. M. Langer, in *New Developments in Semiconductor Physics*, Vol. 122 of *Lecture Notes in Physics*, edited by F. Beleznay, G. Ferenczi, and J. Giber (Springer, New York, 1980), p. 123.

[5]R. J. Nelson, Appl. Phys. Lett. 31, 351 (1977).

[6]D. V. Lang, R. A. Logan, Phys. Rev. B 19, 1015 (1979).

[7]R. A. Craven and D. Finn, J. Appl. Phys. 50, 6334, (1979).

[8]G. Vincent and D. Bois, Solid State Commun. 27, 431 (1978).

[9]G. Vincent, D. Bois, and A. Chantre, J. Appl. Phys. 53, 3643 (1982).

[10]A. Mitonneau and A. Mircea, Solid State Commun. 30, 157 (1979).

[11]G. E. Jellison, J. Appl. Phys. 53, 5715 (1982).

[12]M. Levinson, Phys. Rev. B 28, 3660 (1983).

[13]M. Levinson, J. L. Benton, H. Temkin, and L. C. Kimerling, Appl. Phys. Lett. 40, 990 (1982).

[14]P. W. Anderson, Phys. Rev. Lett. 34, 953 (1975).